

# Polymorphism of Poly(butylene terephthalate) Investigated by Means of Periodic Density Functional Theory Calculations

Alberto Milani\* and Daria Galimberti

Dipartimento di Chimica, Materiali e Ingegneria Chimica "Giulio Natta", Politecnico di Milano, Piazza Leonardo da Vinci, 32, 20133 Milan, Italy

## S Supporting Information

**ABSTRACT:** The conformation and solid state structure of the two  $\alpha$  and  $\beta$  polymorphs of poly(butylene terephthalate) are here studied by means of state-of-the-art first principles calculations, carried out both for the crystals and the infinite one-dimensional chain models. Focusing in details on the debated  $\beta$  form, induced by mechanical deformation, we verified the setting on of an all-trans conformation, as also supported by the simulation of the infrared spectra of the different polymorphs compared to the available experimental spectra. The transition from the  $\alpha$  to the  $\beta$  form is also simulated by applying increasing strains to the infinite polymer chain: a peculiar evolution of the intramolecular structure is indeed predicted, showing a transition from the GTG' conformation found for the  $\alpha$  form to the TTT conformation of the strained  $\beta$  form.

## I. INTRODUCTION

Aromatic polyesters are a class of polymeric materials showing peculiar microstructural properties that can modulate their macroscopic behavior. In this context, phenomena such as different conformational effects and different mechanical behavior for the members of this family, even-odd effects depending on the number of methylene units between aromatic rings, polymorphic transitions among two or more phases etc. are just a few examples. Therefore, despite their technological importance and their widespread application in our everyday life, there are several physicochemical phenomena that still need a complete investigation; furthermore, there are some ambiguities and open questions that still demand an answer.

Poly(butylene terephthalate) (PBT), the second member of this family in order of technological importance after poly(ethylene terephthalate) (PET), shows a reversible transition between different crystal structures upon mechanical deformation, which corresponds to a variation in the conformation of the chain.<sup>1–22</sup> Many authors have investigated this polymorphic transition by means of different characterization techniques, ranging from X-ray diffraction (XRD)<sup>1–6,19,21,22</sup> to electron microscopy,<sup>23</sup> vibrational spectroscopy,<sup>7–10,13–18</sup> nuclear magnetic resonance,<sup>24</sup> and molecular mechanics simulations.<sup>12</sup> Despite this large interest, some features are still debated, such as for example the structure of the polymer in the stress-induced  $\beta$  phase: while most of the authors agree in proposing an all-trans structure, other ones have proposed a different conformation for the PBT chains in the crystal. As for other classes of polymers, both XRD and vibrational spectroscopy techniques have been usually adopted to investigate structural properties but they have been based almost exclusively on experimental works, generating sometimes further ambiguities which cannot be easily unravelled. In these grounds, first-principles computational techniques can give a reliable description of both the structural and vibrational properties of the system, even if, to this aim, the suitable computational tools capable of treating periodic molecular

crystal became available only in very recent years.<sup>25–27</sup> Therefore, in this paper we have applied state-of-the-art techniques to carry out periodic Density Functional Theory (DFT) calculations augmented with an empirical dispersion correction (DFT-D)<sup>28–30</sup> of poly(butylene terephthalate) polymorphs by means of the CRYSTAL09 code,<sup>31,32</sup> to investigate and clarify definitively both the structural and vibrational properties of these systems. Very recently, this code has been applied successfully to many other polymeric systems (polystyrene,<sup>25,26</sup> polyglycine,<sup>27</sup> nylon-6 polymorphs,<sup>33</sup> nylon-6,6,<sup>34</sup> and polytetrafluoroethylene<sup>35</sup>) and we used it also for the spectroscopic characterization of poly(trimethylene terephthalate),<sup>36</sup> another member of the aromatic polyester class.

In the following, after explaining the computational methodology adopted, we will present the simulation of both the intramolecular and solid-state structure of PBT; then we will proceed to the simulation of its IR spectra, compared to the experimental data available in the literature. At last, the effect of the mechanical deformation will be introduced in the calculation to monitor the evolution of the conformation of the infinite polymer chain.

## II. COMPUTATIONAL DETAILS

Full geometry optimization of the crystal structure, chain conformation and the calculation of the IR spectra of PBT have been carried out by means of the CRYSTAL09 code<sup>31,32</sup> in the framework of Density Functional Theory. We adopted the B3LYP<sup>37,38</sup> hybrid exchange-correlation functional with the 6-31G(d,p) basis set, introducing also the empirical correction for dispersion interaction (B3LYP-D) proposed by Grimme<sup>28–30</sup> and implemented in CRYSTAL09. The choice of both the DFT functional and basis set is motivated on the basis of previous computational investigations of polymer systems by means of the CRYSTAL code<sup>25–27,33–35</sup> where it has been found that this combination can give a very good description

**Received:** December 19, 2013

**Revised:** January 14, 2014

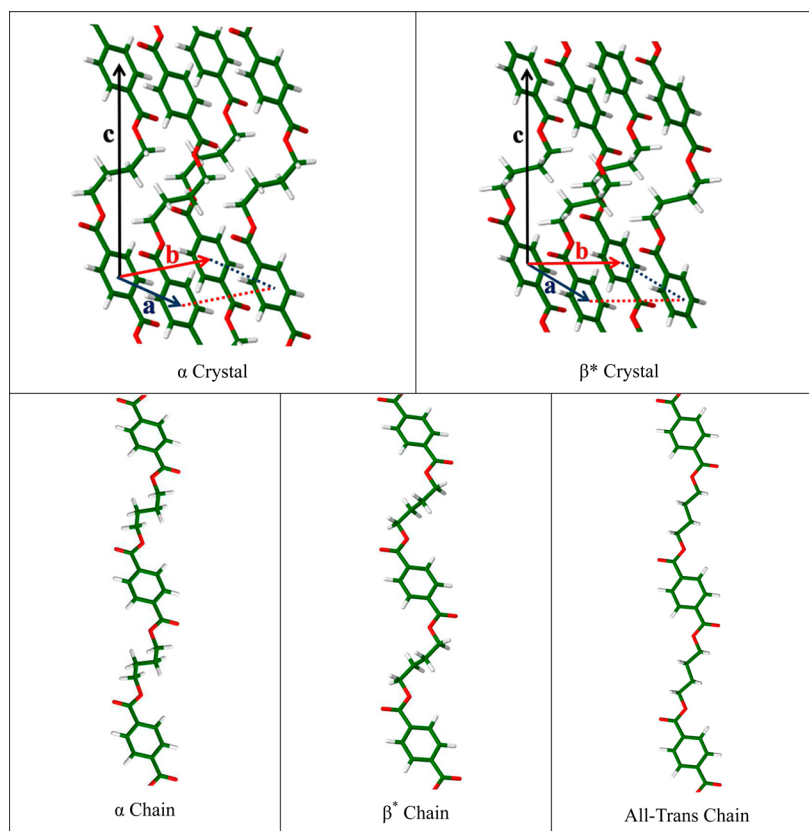
**Published:** January 28, 2014



**Table 1.** Summary of the Numerical Values Adopted for the Parameters Occurring in Grimme's Correction for Dispersion Interactions<sup>a</sup>

$d$	$s_6$	$C_6^H$	$C_6^C$	$C_6^O$	$C_6^N$	$R_{vdw}^H$	$R_{vdw}^C$	$R_{vdw}^O$	$R_{vdw}^N$
20	1.00	0.14	1.75	0.70	1.23	1.3013	1.70	1.52	1.55

<sup>a</sup>A cutoff distance of 25.0 Å was used to truncate direct lattice summation.  $C_6$  are in units of J nm<sup>6</sup> mol<sup>−1</sup> while  $R_{vdw}$  are in unit of Å.

**Figure 1.** Sketches of the optimized  $\alpha$  and  $\beta^*$  crystalline structures of PBT and of the 1D model chains possessing  $\alpha$ ,  $\beta^*$  and trans conformation. For a definition of  $\beta^*$  see section III.1.

of both the structure and the vibrational spectra. Furthermore, in a very recent paper,<sup>36</sup> the case of poly(trimethyl terephthalate) have been investigated by taking into account also the effect of different computational parameters, including both basis set choice and the parameters used for Grimme's corrections: it has been found that B3LYP/6-31G(d,p), combined with the parameters previously adopted for nylon-6 polymorphs<sup>33</sup> and nylon-6,6<sup>34</sup> and reported in Table 1, gives indeed the best agreement with the experimental data. This combination is thus used also in the present study.

In all calculations, the atomic positions and the lattice parameters were fully optimized; default optimization algorithms and convergence criteria were adopted. In the case of PBT, two polymorphs have been characterized by different authors:<sup>1–6,19,21</sup> the  $\alpha$  form is the stable one found in the unstrained condition and it shows a GGTG'/G' conformation on the O–CH<sub>2</sub> bonds and on the methylene chain. The structural determinations proposed by different authors are in agreement about both the crystal and conformational structure. A second polymorph  $\beta$  is observed for PBT under strain. In this case, non-negligible discrepancies are found among different authors: while Yokouchi et al.<sup>1</sup> report a TSTS'T conformation, many other authors<sup>4–6,12,19,22</sup> propose an all-trans conformation for the methylene chains in  $\beta$  phase. In all the cases, both the polymorphs have a triclinic unit cell with  $P\bar{1}$  space group.

Since Cartesian coordinates of both phases are reported only by Yokouchi et al.,<sup>1</sup> we used these geometries as initial guess for the full geometry optimization of  $\alpha$  and  $\beta$  crystals. In addition to the simulation of the whole crystal, we carried out also simulations for

infinite polymer chains (1D model chain); in this case, three structures have been taken into account as starting geometries: the two structures having the conformations observed in  $\alpha$  and  $\beta$  crystals and the all-trans chain.

The optimized structures of all these crystals and 1D model chains are sketched in Figure 1.

In all the cases, normal frequencies calculations at the  $\Gamma$  point have been carried out on the optimized geometries as achieved by diagonalization of the (numerically calculated) Hessian matrix.

The DFT-D computed spectra have been compared with the available experimental IR spectra reported by Stambaugh et al.<sup>7</sup> To compare the computed and the experimental data, the calculated frequencies were scaled by 0.9748: this scaling factor has been determined to put the band computed at 940.7 cm<sup>−1</sup> for the 1D model chain of the  $\alpha$  polymorph in correspondence of the well-assessed marker band found at 917 cm<sup>−1</sup> for the  $\alpha$  form.

In addition to the geometry optimization and the prediction of the IR spectra, we also simulate the effect of the mechanical deformation on the conformational structure of a single infinite PBT chain: starting from the geometry of the chain in  $\alpha$  conformation ( $c' = 23.0166$  Å, chain repeat distance) we progressively increased the value of the repeat distance  $c'$  by steps of 0.2 Å until a final value of 28 Å. For each step, a geometry optimization at fixed  $c'$  has been carried out and the final structure of each step has been used as input for the next one. The evolution of the conformation has been thus followed for increasing strain to verify the occurrence of the polymorphic transition from the  $\alpha$  to the all-trans  $\beta$  conformation.

**Table 2. Comparison between DFT-D Computed (B3LYP-D/6-31G(d,p)) Cell Parameters and Those Reported in Previous Investigations for the  $\alpha$  Phase of PBT<sup>a</sup>**

$\alpha$ -PBT	B3LYP-D/6-31G(d,p)	MM <sup>12</sup>	expt <sup>1</sup>	expt <sup>2</sup>	expt <sup>3</sup>	expt <sup>4</sup>	expt <sup>6</sup>	expt aver. <sup>6</sup>	errors (%)
<i>a</i>	4.5812	5.343	4.83	4.83	4.87	4.89	4.87	4.86	−5.7
<i>b</i>	5.8684	6.340	5.94	5.96	5.96	5.95	5.99	5.96	−1.5
<i>c</i>	11.8396	10.631	11.59	11.62	11.71	11.67	11.67	11.65	1.6
$\alpha$	101.0030	98.220	99.70	99.90	100.10	98.90	99.80	99.70	1.3
$\beta$	114.2940	117.130	115.20	115.20	116.60	116.60	116.20	116.00	−1.5
$\gamma$	111.0675	114.320	110.80	111.30	110.30	110.90	110.90	110.80	0.2

<sup>a</sup>Values of *a*, *b*, *c* parameters are in Å and in degrees for the angles. In the last column, the percentage errors (%) of the DFT-D computed values and the average experimental one reported by Desborough et al.<sup>6</sup> are calculated.

**Table 3. Comparison between DFT-D Computed (B3LYP-D/6-31G(d,p)) Cell Parameters and Those Reported in Previous Investigations for the  $\beta$  Phase of PBT<sup>a</sup>**

$\beta$ -PBT	B3LYP-D 6-31G(d,p)	MM <sup>12</sup>	expt <sup>1</sup>	expt <sup>4</sup>	expt <sup>6</sup>
<i>a</i>	4.7421	4.874	4.95	4.69	4.73
<i>b</i>	5.9071	6.053	5.67	5.80	5.83
<i>c</i>	12.1937	13.048	12.95	13.00	12.90
$\alpha$	97.8208	104.650	101.70	101.90	101.90
$\beta$	125.9010	125.040	121.80	120.50	119.40
$\gamma$	101.5888	103.060	99.90	105.00	105.10

<sup>a</sup>Values of *a*, *b*, *c* parameters are in Å and in degrees for the angles. Since different structures have been experimentally resolved, no reference experimental cell parameters can be unambiguously defined to calculate percentage errors with respect to the DFT-D computed data.

### III. RESULTS AND DISCUSSION

#### III.1. Structure and Conformation of PBT Polymorphs.

In Tables 2 and 3, we report the comparison between our computational results and the previous determinations of the crystal structure of  $\alpha$  and  $\beta$  polymorphs; a comparison between the conformations observed in the two polymorphs is reported respectively in Tables 4 and 5.

A very good agreement is obtained for the  $\alpha$  form. In the last column of Table 2, we report the percentage errors of our DFT-D computed cell parameters with respect to the experimental average parameters reported by Desborough et al.<sup>6</sup> all the errors are very small and the largest discrepancy is found for the parameter *a*, ruling the van der Waals packing of neighbor chains. This parameter is indeed largely affected by

**Table 5. Comparison between DFT-D computed (B3LYP-D/6-31G(d,p)) torsional angles and those reported in previous investigations for the  $\beta$  phase of PBT. A sketch is reported in Table 4 for the definition of these angles. Values are in degrees**

$\beta$ -PBT	B3LYP-D 6-31G(d,p)	MM <sup>12</sup>	expt <sup>1</sup>	expt <sup>4</sup>	expt <sup>22</sup>
$\tau_1$ (CCOC)	180	−129	179	−179	−179
$\tau_2$ (COCC)	179	175	−179	−159	−159
$\tau_3$ (OCCC)	71	177	113	162	−166
$\tau_4$ (CCCC)	180	180	180	180	180

the parameters chosen for Grimme's correction from one hand and by temperature effects that are not present in our simulation on the other hand, as also pointed out in previous works.<sup>33,34</sup> In any case, the absolute deviation of the DFT-D value from the experimental one is small (0.28 Å). If we compare our DFT-D results with the cell parameters computed by Nitsche et al.<sup>12</sup> by means of molecular mechanics (MM) simulations (second column of Table 2) we can verify that DFT-D calculations give a better agreement with the experiments, even if the effect of temperature is not included. This is true in particular for the *c* parameter (chain repeat distance), underestimated by about 1 Å by MM simulations and overestimated only by 0.19 Å by our calculations. In any case, it should be noted that all the data reported for the  $\alpha$  form show a very good agreement. Such an accordance is also found when considering the conformation of the chain (Table 4): all the authors indeed propose a GG'G'G' sequence on the O−CH<sub>2</sub> bonds and on the methylene chain and again our calculations predict values of the torsional angles which are very close to the experimental ones, in particular to the angles reported in refs 2

**Table 4. Comparison between DFT-D Computed (B3LYP-D/6-31G(d,p)) Torsional Angles and Those Reported in Previous Investigations for the  $\alpha$  Phase of PBT<sup>a</sup>**

$\alpha$ -PBT					
	B3LYP-D 6-31G(d,p)	MM <sup>12</sup>	expt <sup>1</sup>	expt <sup>4</sup>	expt <sup>2</sup>
$\tau_1$ (CCOC)	180	152	178	−178	178
$\tau_2$ (COCC)	−94	−68	−88	−94	−91
$\tau_3$ (OCCC)	−67	−61	−66	−79	−88
$\tau_4$ (CCCC)	180	180	180	180	180

<sup>a</sup>A sketch is also reported for the definition of these angles. Values are in degrees.

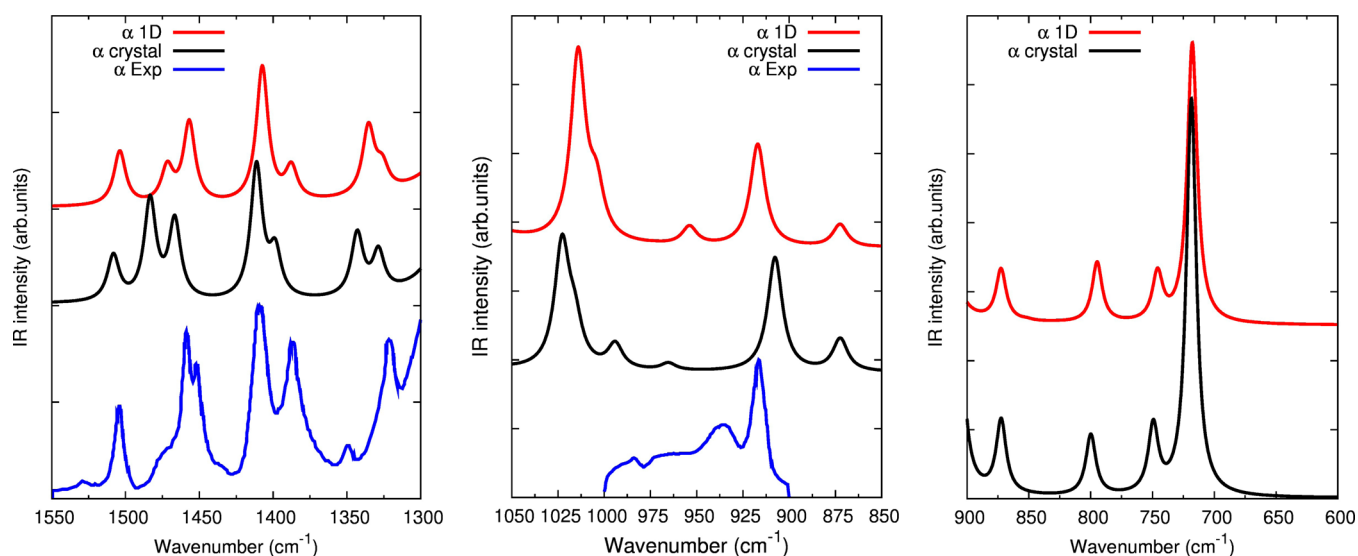


**Figure 2.** Comparison of DFT-D computed (B3LYP-D/6-31G(d,p)) IR spectra of the crystal and of the infinite polymer chain (1D model chain) of the  $\alpha$  phase with the experimental spectra reported in ref 7. The computed frequencies are scaled by 0.9748.

and 4. Also, in this case, our accuracy is larger with respect to MM simulations, where  $\tau_1$  and  $\tau_2$  angles in particular show a non-negligible difference from the experimental data.

In the case of the  $\beta$  phase, differences are found among the various authors (see Tables 3 and 5): most of them<sup>4–6,12,19,22</sup> agree in proposing an all-trans conformation for this phase, contrary to the previous proposal to TSTS'T by Yokouchi et al.<sup>1</sup> ( $\tau_3 = 113^\circ$ ). MM simulations<sup>12</sup> predict cell parameters in good agreement with refs 4 and 6 and confirm a trans conformation on the central methylene units, even if a value of  $-129^\circ$  is anyway computed for  $\tau_1$  contrary to the T angles experimentally observed by all the other authors.

In this context, our calculation predicts a further new equilibrium structure; indeed, a TGTG'T is computed ( $\tau_3 = -71^\circ$ ) which is different from all the previous proposals, both from the all-trans structure and the conformation containing skew torsional angles. Our chain is thus more contracted, resulting in a smaller  $c$  parameter, in our case equal to 12.194 Å, contrary to the experimental values of about 13 Å. Because of this difference and to avoid any confusion, from now on we will indicate our DFT-D optimized structure as  $\beta^*$  form.

In order to clarify in deeper details these differences, we carried out DFT-D calculation also for 1D model chains, i.e. single infinite polymer chains possessing the conformation observed in  $\alpha$  and  $\beta^*$  crystals and also all-trans conformation. In the case of the “ $\alpha$  chain” and of the “ $\beta^*$  chain” torsional angles of  $178^\circ$ ,  $85^\circ$ ,  $57^\circ$ ,  $159^\circ$  and  $178^\circ$ ,  $167^\circ$ ,  $-68^\circ$ ,  $180^\circ$ , respectively, are found, thus giving the same conformation observed also in the crystal and excluding the role of any intermolecular effect in modulating the intramolecular structure of the polymer.

Further information can be obtained by calculating the relative energies of the two phases: as expected the  $\beta^*$  crystal is less stable by 3.86 kcal/mol (referred to the unit cell, 56 atoms) with respect to the  $\alpha$  form. When considering the infinite chains, this value becomes 2.29 kcal/mol, thus showing that both the intramolecular structure and the intermolecular packing are energetically more efficient in the  $\alpha$  form. Interestingly, the all-trans chain is less stable by 3.61 kcal/mol with respect to the  $\alpha$  chain and it appears to be also less stable with respect to the  $\beta^*$  chain. However, to give a more

reliable description of the structural evolution of the conformation upon mechanical deformation, we need to include explicitly the effect of the strain in our simulation, as described in section III.3 and which introduces a perturbation with respect to 1D model chains treated as completely isolated systems.

On the basis of the computational study here reported, we are not able yet to confirm any of the previous proposal for the structure of the  $\beta$  polymorph; moreover, based on our first-principles calculations the conformational properties of PBT seems to be even more complicated. In order to solve all these discrepancies, we need to take into account also other properties of PBT: the vibrational properties are the ideal ground to obtain other structural information, due to the extreme sensitivity of IR and Raman spectra to both intra- and intermolecular phenomena. Indeed, also in previous papers,<sup>25–27,33–35</sup> IR spectroscopy has been widely used to this aim and we demonstrated how the computational method adopted in the current work is very powerful and allows to answer many open questions concerning the spectroscopic characterization of different polymers, including PTT. Also in the case of PBT, no computational studies have been reported yet about the interpretation of the vibrational properties and the assignment of its IR spectrum. In the next section, we will verify that the comparison between experimental and DFT-D computed spectra will allow to clarify which is the structure of the so-debated  $\beta$  polymorph.

**III.2. IR Spectroscopy of PBT Polymorphs.** As a first step in the analysis of the spectra of PBT we have to check if our DFT-D calculations can give a reliable prediction of the IR spectra. To this aim, in Figure 2, we compare the spectra computed for the crystal and the 1D model chain of the  $\alpha$  phase with the experimental spectra reported by Stambaugh et al.<sup>7</sup> The agreement between the experimental and DFT-D spectra is good and demonstrate the reliability of the computational method adopted. By looking in particular to the first panel, we can verify that the experimental pattern is correctly described by the calculation on the crystal, both in frequency and relative intensity. The 1D model chain shows IR spectra which are very similar to the crystal and the only discrepancy that occurs concerns the relative intensity of the



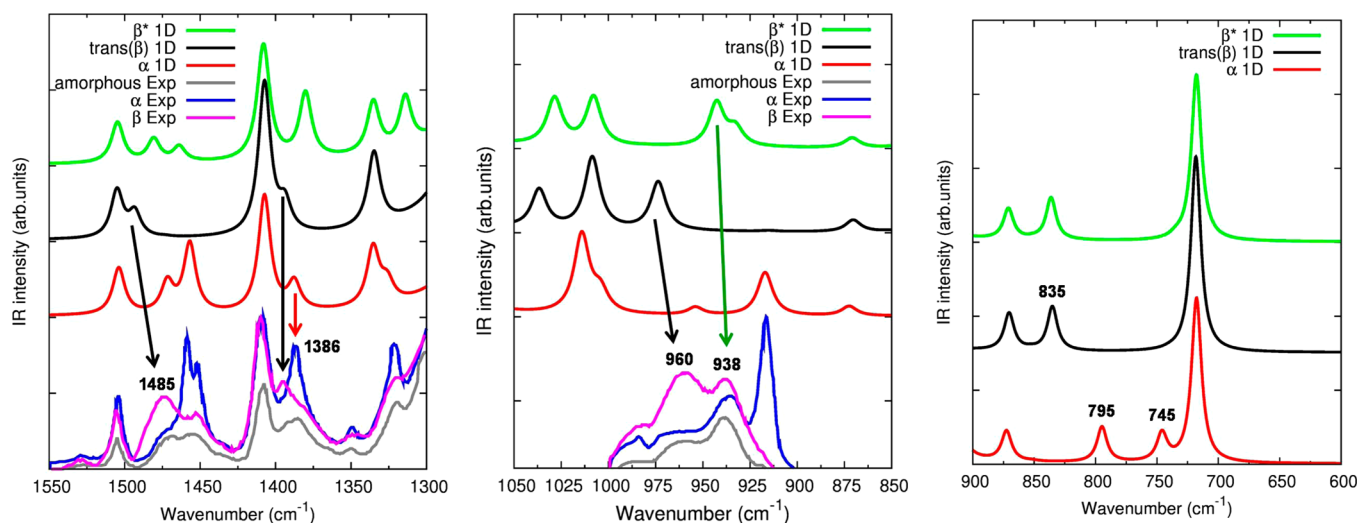


**Figure 3.** Comparison of DFT-D computed (B3LYP-D/6-31G(d,p)) IR spectra of the 1D chain models ( $\alpha$ ,  $\beta^*$ , and trans conformations) with the experimental spectra reported in ref 7 for both polymorphs and the amorphous phase. The computed frequencies are scaled by 0.9748.

**Table 6.** Experimental and DFT-D Computed (B3LYP-D/6-31G(d,p)) Frequency Values in  $\text{cm}^{-1}$  of the Most Important Bands of  $\alpha$ ,  $\beta$ , and Amorphous Phase of PBT<sup>a</sup>

PBT $\alpha$ phase			PBT $\beta$ phase					amorphous
expt <sup>7-10,13-18</sup>	1D chain B3LYP-D/6-31G (d, p)		expt <sup>7-10,13-18</sup>	1D all-trans chain B3LYP-D/6-31G (d, p)		1D $\beta^*$ chain B3LYP-D/6-31G (d, p)		expt <sup>7-10,13-18</sup>
	frequency (scaled by 0.9748) (cm <sup>-1</sup> )	IR intensity (km/mol)		frequency (scaled by 0.9748) (cm <sup>-1</sup> )	IR intensity (km/mol)	frequency (scaled by 0.9748) (cm <sup>-1</sup> )	IR intensity (km/mol)	
1460	1472	29	1485	1493	19	1481	22	
1455	1457	64	1470			1464	13	
1386	1388	25	1393	1394	22	1381	60	1386, 1375
1350	1336	56	960	974	98			
1323	1326	20				943	101	938
917	917	105				933	40	
811	795	27	845	835	28	836	31	
750	745	22						

<sup>a</sup>The computed frequencies refer to the 1D chain models ( $\alpha$ ,  $\beta^*$ , and trans conformations) and they are scaled by 0.9748. Computed IR intensities (km/mol) are also reported.

two bands predicted at about  $1450\text{ cm}^{-1}$  ( $\text{CH}_2$  bending modes). Excluding this minor detail, both calculations reproduce the same pattern: on these grounds, from now on, we will compare the experimental spectra with the computational spectra of the 1D model chains, to obtain a clearer and simpler interpretation of the structural properties of PBT polymorphs on the basis of their conformation.

In Figure 3, the IR spectra computed for the 1D model chains having respectively  $\alpha$ ,  $\beta^*$  and trans conformation are compared with the experimental spectra of both polymorphs and of the amorphous phase, and in Table 6 the experimental frequency values of the main marker bands are compared to the DFT-D computed values. In the Supporting Information, the sketches of the computed normal modes of vibration are reported for each one of these bands.

The frequency range which have been mostly used to investigate PBT polymorphism is the  $900\text{--}1000\text{ cm}^{-1}$  region. The band at  $917\text{ cm}^{-1}$  (COCC torsional + CH deformation mode) has been unambiguously associated with the  $\alpha$  phase and it has been used in the present work as a reference to determine the frequency scaling factor for all the computed spectra (see Computational Details). In addition to this band, the  $\alpha$  form shows also a second broad band at  $938\text{ cm}^{-1}$ : based

on the comparison with the spectrum of the amorphous phase we can verify that this band is due only to the amorphous, which is present in a non-negligible amount. This fact is indeed supported by the computed spectrum where no bands are predicted in correspondence of this peak for the  $\alpha$  phase. In the case of the  $\beta$  polymorph, the experimental spectra clearly show the occurrence of a new band at  $960\text{ cm}^{-1}$  in addition to the band at  $938\text{ cm}^{-1}$  (the latter one demonstrating again the presence of a non-negligible amount of amorphous phase). It is now immediate to verify from the comparison with the DFT-D computed spectra that the model chain describing the occurrence of this marker band at  $960\text{ cm}^{-1}$  is actually the trans chain (band computed at  $974\text{ cm}^{-1}$ , CO stretching + COC bending +  $\text{CH}_2$  deformation mode), confirming definitely that the  $\beta$  phase of PBT does possess chains in transplanar conformation.

It is interesting to note that the chain possessing the  $\beta^*$  conformation has a doublet of bands in correspondence of the  $938\text{ cm}^{-1}$  experimental band: based on the eigenvectors sketched in the Supporting Information, we can indeed verify that these vibrations are located on the methylene units where one G torsional angle is present. On these grounds, we can assume that the 1D model chain in  $\beta^*$  conformation could be

considered as a representative of the several possible conformers, populated in the amorphous phase, possessing one TGT sequence somewhere on the methylene chain.

By analyzing now the 1550–1300  $\text{cm}^{-1}$  frequency region further information is obtained. First of all, based on the DFT-D calculation, we confirm again that the doublet of bands observed at 1460/1455  $\text{cm}^{-1}$  in the experimental spectra is associated with the  $\alpha$  phase. In this case, the relative intensities of the two components are not predicted correctly by the calculations: in Figure 2, we have already pointed out that this is the only deficiency observed for the 1D model chain, since the spectrum computed for the  $\alpha$  crystal reproduces very well the relative intensity of this doublet. The experimental spectra reveal that the amorphous gives two broad bands in this region: in the case of the  $\beta^*$  chain two peaks are indeed predicted in correspondence of these two features, thus supporting again the assumption that this model can be taken as a representative of the amorphous phase.

In the case of the  $\beta$  polymorph, a marker band is now observed at 1485  $\text{cm}^{-1}$ , which is again nicely predicted by the transplanar chain model (band computed at 1493  $\text{cm}^{-1}$ ,  $\text{CH}_2$  bending mode).

Further differences are also observed at about 1390  $\text{cm}^{-1}$ : the  $\alpha$  and  $\beta$  phase show two bands at about 1386 and 1393  $\text{cm}^{-1}$  respectively. The  $\alpha$  chain model and the trans chain model actually possess two bands at 1388 and 1394  $\text{cm}^{-1}$  ( $\text{CH}_2$  deformation modes) in very nice agreement with the experiments; in this region, the amorphous presents a broad band at about 1385–1380  $\text{cm}^{-1}$ , predicted at 1381  $\text{cm}^{-1}$  by the  $\beta^*$  model.

At last, even if no experimental spectra are available, we report in the last panel of Figure 3 the comparison of the IR spectra of the different 1D chain models in the 900–600  $\text{cm}^{-1}$  range. In the previous literature two marker bands are here found at 811 and 750  $\text{cm}^{-1}$  for the  $\alpha$  phase and a band at 845  $\text{cm}^{-1}$  for the  $\beta$  phase: DFT-D computed spectra show indeed the two corresponding marker bands at 795  $\text{cm}^{-1}$  (OCO bending + CH deformation mode) and 745  $\text{cm}^{-1}$  ( $\text{CH}_2$  deformation mode) for the  $\alpha$  chain and at 835  $\text{cm}^{-1}$  (OCO bending + CH deformation mode) for the trans chain.

As a conclusion, thanks to computational vibrational spectroscopy, we have been able to demonstrate unambiguously that the  $\beta$  polymorph of PBT possess chains in transplanar conformation.

**III.3. Simulation of the  $\alpha \rightarrow \beta$  Transition.** In this section, we investigate in more details the structural evolution of a PBT chain in  $\alpha$  conformation for increasing value of the strain. This has been simulated by increasing step by step the values of the  $c'$  parameter of the chain and reoptimizing the geometry each step to monitor the changes of the conformation. The results are reported in Figure 4, showing the evolution of the torsional angles for increasing strain.

Only small changes are observed until about a strain of 14%: at this value, the  $\tau_3$  angle suddenly jumps from about 80° to about 170°, that is it evolves from the G toward the T conformation while  $\tau_2$  angle still remains stable at about 90°. If we further increase the strain, at about  $\varepsilon = 19\%$  also  $\tau_2$  angle shows a transition to the T conformation and the whole chain now possesses an all-trans structure.

The use of periodic boundary conditions in the calculation usually implies some difficulties and restraints for the conformational transitions; therefore, we cannot state that the transition is really a two-step evolution of the  $\tau_2$  and  $\tau_3$  angles.

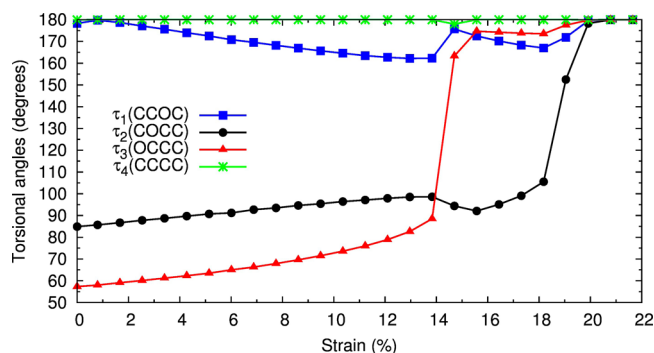


**Figure 4.** Evolution of the B3LYP-D/6-31G(d,p) computed torsional angles on the methylene chain (see Table 2 for the definition of the angles) for increasing values of the strain of the 1D model chain of the  $\alpha$  phase. The strain is calculated as  $(c' - c'_0) \times 100/c'_0$ , where  $c'_0$  is the optimized cell parameter of the  $\alpha$  chain while  $c'$  is progressively increased to simulate the mechanical deformation. The numerical values of these torsional angles as a function of  $c'$  are reported in the Supporting Information.

In any case, it is clearly demonstrated again that the transition from the  $\alpha$  to the  $\beta$  phase upon mechanical deformation does imply an evolution of the chain structure from the GGTG'G' to the all-trans conformation.

#### IV. CONCLUSIONS

Thanks to state-of-the-art computational methods, we have been able to investigate in details the crystal phase transition observed in PBT under mechanical deformation. DFT-D calculations allowed to solve unambiguously the discrepancies found in the literature about the nature of the  $\beta$  phase: our study reveals that this phase is characterized by an all-trans chain conformation, promoted by increasing values of the strain. This has been possible by simulating the crystal structure of the different phases of PBT and by computing their IR spectra, compared to the experimental ones: indeed the simulation of these properties is a powerful tool to support and explain the experimental data, free from any ambiguity. The results so obtained demonstrate that accurate first-principles calculations of crystalline polymers are now possible and can be applied to discuss a wide range of problems, providing answers to several open questions where experimental characterizations are not enough. Their importance is not restricted to the interpretation of the chemical/physical properties of polymers but they could be also a valuable tool in the development and characterization of innovative systems or for the design of new polymeric materials.

#### ■ ASSOCIATED CONTENT

##### Supporting Information

Sketches of the main IR active modes for PBT chain ( $\alpha$ , all-trans,  $\beta^*$ ), table with DFT-D computed torsional angles of the methylene chain for increasing value of the  $c'$  parameter of  $\alpha$ -PBT 1D model chain, tables with DFT-D optimized values of the cell parameters and fractional atomic coordinates obtained by full optimization of the cell of PBT  $\alpha$  and  $\beta^*$  crystal, tables with DFT-D optimized values of the cell parameter and Cartesian atomic coordinates obtained by full optimization of the cell of the single polymeric chain (1D crystal) of  $\alpha$ , all-trans, and  $\beta^*$  PBT chain, and tables with DFT-D computed values of frequencies ( $\text{cm}^{-1}$ ) and IR intensities ( $\text{km/mol}$ ) for the PBT  $\alpha$ ,

all-trans,  $\beta^*$  chain, and  $\alpha$  and  $\beta$  crystals. This material is available free of charge via the Internet at <http://pubs.acs.org/>.

## AUTHOR INFORMATION

### Corresponding Author

\*(A.M.) E-mail: [alberto.milani@polimi.it](mailto:alberto.milani@polimi.it).

### Notes

The authors declare no competing financial interest.

## REFERENCES

- (1) Yokouchi, M.; Sakakibara, Y.; Chatani, Y.; Tadokoro, H.; Tanaka, T.; Yoda, K. *Macromolecules* **1976**, *9*, 266–273.
- (2) Mencik, Z. *J. Polym. Sci., Polym. Phys. Ed.* **1975**, *13*, 2173–2181.
- (3) Joly, A. M.; Nemoz, G.; Douillard, A.; Vallet, G. *Makromol. Chem.* **1975**, *176*, 479–494.
- (4) Hall, I. H.; Pass, M. G. *Polymer* **1976**, *17*, 807–816.
- (5) Stambaugh, B.; Koenig, J. L.; Lando, J. B. *J. Polym. Sci., Polym. Phys. Ed.* **1979**, *17*, 1053–1062.
- (6) Desborough, I. J.; Hall, I. H. *Polymer* **1977**, *18*, 825–830.
- (7) Stambaugh, B.; Lando, J. B.; Koenig, J. L. *J. Polym. Sci., Polym. Phys. Ed.* **1979**, *17*, 1063–1071.
- (8) Siesler, H. W. *Makromol. Chem.* **1979**, *180*, 2261–2263.
- (9) Stambaugh, B. D.; Koenig, J. L.; Lando, J. B. *J. Polym. Sci., Polym. Lett. Ed.* **1977**, *15*, 299–303.
- (10) Jakeways, R.; Smith, T.; Ward, I. M.; Wilding, M. A. *J. Polym. Sci., Polym. Lett. Ed.* **1976**, *14*, 41–46.
- (11) Jakeways, R.; Ward, I. M.; Wilding, M. A.; Hall, I. H.; Desborough, I. J.; Pass, M. G. *J. Polym. Sci., Polym. Phys. Ed.* **1975**, *13*, 799–813.
- (12) Nitzsche, S. A.; Wang, Y. K.; Hsu, S. L. *Macromolecules* **1992**, *25*, 2397–2400.
- (13) Roebuck, J.; Jakeways, R.; Ward, I. M. *Polymer* **1992**, *33*, 227–232.
- (14) Gillette, P. C.; Lando, J. B.; Koenig, J. L. *Polymer* **1985**, *26*, 235–240.
- (15) Siesler, H. W. *J. Polym. Sci., Polym. Lett. Ed.* **1979**, *17*, 453–458.
- (16) Ward, I. M.; Wilding, M. A. *Polymer* **1977**, *18*, 327–335.
- (17) Dobrovolnyarand, E.; Hsu, S.; Shih, C. *Macromolecules* **1987**, *20*, 1022–1029.
- (18) Stach, W.; Holand-Moritz, K. *J. Mol. Struct.* **1980**, *60*, 49–54.
- (19) Kawaguchi, A.; Murakami, S.; Fujiwara, M.; Nishikawa, Y. *J. Polym. Sci., Part B: Polym. Phys.* **2000**, *38*, 838–845.
- (20) Takahashi, Y.; Murakami, K.; Nishikawa, S. *J. Polym. Sci., Part B: Polym. Phys.* **2002**, *40*, 765–771.
- (21) Apostolov, A. A.; Fakirov, S.; Stamm, M.; Patil, R. D.; Mark, J. E. *Macromolecules* **2000**, *33*, 6856–6860.
- (22) Grasso, R. P.; Perry, B. C.; Koenig, J. L.; Lando, J. B. *Macromolecules* **1989**, *22*, 1267–1272.
- (23) Roche, E. J.; Stein, R. S.; Thomas, E. L. *J. Polym. Sci., Polym. Phys. Ed.* **1980**, *18*, 1145–1158.
- (24) Davidson, I. S.; Manuel, A. J.; Ward, I. M. *Polymer* **1983**, *24*, 30–36.
- (25) Torres, F. J.; Civalleri, B.; Meyer, A.; Musto, P.; Albunia, A. R.; Rizzo, P.; Guerra, G. *J. Phys. Chem. B* **2009**, *113*, 5059–5071.
- (26) Torres, F. J.; Civalleri, B.; Pisani, C.; Musto, P.; Albunia, A. R.; Guerra, G. *J. Phys. Chem. B* **2007**, *111*, 6327–6335.
- (27) Ferrari, A. M.; Civalleri, B.; Dovesi, R. *J. Comput. Chem.* **2010**, *31*, 1777–1784.
- (28) Civalleri, B.; Zicovich-Wilson, C. M.; Valenzano, L.; Ugliengo, P. *CrystEngComm* **2008**, *10*, 405–410.
- (29) Grimme, S. *J. Comput. Chem.* **2004**, *25*, 1463–1473.
- (30) Grimme, S. *J. Comput. Chem.* **2006**, *27*, 1787–1799.
- (31) Dovesi, R.; Orlando, R.; Civalleri, B.; Roetti, C.; Saunders, V. R.; Zicovich-Wilson, C. M. *Z. Kristallogr.* **2005**, *220*, 571–573.
- (32) Dovesi, R.; Saunders, V. R.; Roetti, C.; Orlando, R.; Zicovich-Wilson, C. M.; Pascale, F.; Civalleri, B.; Doll, K.; Harrison, N. M.; Bush, I. J.; D'Arco, P.; Llunell, M. *CRYSTAL09 User's Manual*; University of Torino: Torino, 2009.
- (33) Quarti, C.; Milani, A.; Civalleri, B.; Orlando, R.; Castiglioni, C. *J. Phys. Chem. B* **2012**, *116*, 8299–8311.
- (34) Galimberti, D.; Quarti, C.; Milani, A.; Brambilla, L.; Civalleri, B.; Castiglioni, C. *Vib. Spectrosc.* **2013**, *66*, 83–92.
- (35) Quarti, C.; Milani, A.; Castiglioni, C. *J. Phys. Chem. B* **2013**, *117*, 706–718.
- (36) Galimberti, D.; Milani, A. Submitted for publication.
- (37) Becke, A. *J. Chem. Phys.* **1993**, *98*, 5648–5652.
- (38) Lee, C.; Yang, W.; Parr, R. *Phys. Rev. B* **1988**, *37*, 785–789.